

THE POSSIBILITY OF APPLICATION OF PYROMETRIC METHOD IN INDUSTRIAL DOSIMETRY OF ELECTRON BEAM RADIATION

R.I. Pomatsalyuk, S.K. Romanovsky, V.A. Shevchenko, A.Eh. Tenishev, D.V. Titov, V.L. Uvarov, A.A. Zakharchenko, V.Ph. Zhyglo

*National Science Center "Kharkov Institute of Physics and Technology", Kharkiv, Ukraine
E-mail: rompom@kipt.kharkov.ua*

Validation of process of medical product sterilization includes absorbed dose mapping in a phantom made of material representative of the object to be processed. Commonly, such measurements are carried out using the disposable chemical dosimeters placed in the phantom at the nodes of the 3D grid. Such a procedure is very laborious and costly in terms of the consumption of dosimeters. In the work, we investigated the possibility of using pyrometric method for prompt mapping of the absorbed dose. The studies were carried out using a rectangular phantom in the form of a set of expanded polystyrene plates, which is exposed to a scanned electron beam. The temperature and absorbed dose distributions in the phantom were measured. A linear dependence between them has been established. The calculation of the absorbed dose profile was also performed by MC simulations. Satisfactory agreement of the calculated dose distribution with the measured one is shown. The limitations of applicability of the proposed method are determined.

PACS: 07.05.Tp; 29.27.-a; 81.40.Wx

INTRODUCTION

Radiation sterilization of medical devices relates to technologies with high degree of responsibility. Its validation under the conditions of a specific radiation facility is carried out in accordance with the ISO 11137-1:2006/Amd 2:2018 standard [1]. One of the stages of validation is the qualification of the operating equipment. It includes irradiation in a specified mode of a homogeneous object (phantom) representative to the sterilized product, and measuring of the spatial distribution of the absorbed dose (dose mapping) in it in accordance with the standard ISO/ASTM 52303:2015 [2]. This procedure, in addition to confirming the characteristics of the radiation, also allows one to check the accuracy of the software product used to simulate and optimize the irradiation mode [3]. Since the main volume of sterilized products is made up of materials with average density of $\sim 10^2$ kg/m³ (dressings, clothing, coatings, etc.), expanded polystyrene (EPS) with a close density was chosen as the phantom material. Its advantage is also high radiation resistance, that enables multiple reuse of the phantom without changing its characteristics [3].

The mapping procedure involves the placement of a large number of disposable dosimeters at the nodes of a 3-dimensional grid in the phantom. Therefore, it is very laborious and costly in terms of consumption of dosimeters and execution time. This is particularly true when the radiation source is an electron accelerator, which parameters determining the dose distribution may vary within wide limits.

The purpose of this paper is to study the conditions of application of pyrometry technique using the thermal imager for operational mapping of the absorbed dose in the phantom.

1. CALORIMETRIC DOSIMETRY OF ELECTRON RADIATION

In technological dosimetry of electron radiation, the calorimetric method with the use of polystyrene (PS) as a material for the sensitive volume of the dosimeter is

used [4]. The advantage of PS, in addition to high radiation resistance, is also its low thermal conductivity.

The method is based on establishing the average value of the absorbed dose D in the sensitive volume from the temperature difference after irradiation T_1 and before it T_0 using the expression:

$$D = (T_1 - T_0) \cdot C(T_1, T_0), \quad (1)$$

where C is the heat capacity of the PS, depending on temperature [5]. Commonly, this dependence is presented in a linearized form:

$$C(T_1, T_0) = C(T_0) + K \cdot \left(\frac{T_1 + T_0}{2} \right), \quad (2)$$

where K – is the coefficient determined during calibration of the dosimeter.

The heat capacity of PS is $\sim 10^3$ J/kg·deg. Thus, the sensitivity of the PS calorimeter dosimeter makes ~ 1 deg/kGy.

In the calorimetric dosimetry, the temperature measurement is usually carried out in off-line mode with a time delay Δt of several minutes, which corresponds to the dosimeter transfer from the irradiation zone to a measuring device. Therefore, the uncertainty of the absorbed dose measurement depends on the accuracy of restore the temperature T_1 . The problem can be solved by fitting the cooling process when the condition

$$\Delta t \ll \tau_c, \quad (3)$$

where τ_c is the cooling constant.

If the condition (3) is satisfied when mapping the dose in the phantom, then its distribution can in principle be reconstructed from the temperature profile in different planes inside the phantom. Such measurements are provided by modern infrared (IR) cameras (thermal imagers) at a temperature error of $\sim 0.1^\circ\text{C}$. In terms of the absorbed dose, this corresponds to $\sim 10^2$ Gy. The dose value usually realized in the technological processes (for example, during sterilization) is about 10 kGy. Therefore, it can be expected that the error in dose determination by the pyrometric method does not exceed a few percent. This is quite enough for adequate reproduction of the dose distribution in the phantom volume.

1.1. THERMAL MODEL OF PS-CALORIMETRIC DOSIMETER

From the point of view of reconstructing the temperature distribution inside the irradiated calorimeter, the problem is reduced to solving a nonstationary heat conduction equation with a given initial distribution determined by the absorbed dose profile and nonlinear boundary conditions. The task is complicated by the lack of accurate data on the thermophysical parameters of both PS and its foam modifications, as well as their dependence on temperature and manufacturing technology [6].

For a semiquantitative analysis of the factors determining the cooling constant, consider a simplified thermal model of a standard PS absorbed dose calorimeter (Fig. 1). It consists of a working medium (capsule) 1 in the form of a PS disk with a density of 854 kg/m³ and a mass of 230 g. The capsule is surrounded by a rectangular heat-insulating shield 2 made of expanded polystyrene with dimension 29×29×10 cm. The density of EPS is 24 kg/m³, weight is 190 g. The shield consists of two parts. The working medium is tightly set in one part, and the second part (cover) can be removed, providing access to it. Inside the working medium there is a thermistor with contacts brought out to the protection surface and calibrated with accuracy of 0.01°C. This design of the calorimeter allows it to be used to compare the temperature of the working media measured with the thermistor and an IR camera.

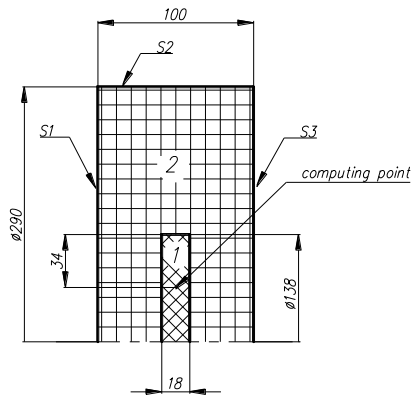


Fig. 1. Structure of the PS-calorimetric dosimeter [4]

Consider a simplified thermal model of a PS calorimeter. Taking into account that the surface density of its thermal insulation at the surface of the capsule is no more than 10% of the surface density of the capsule itself, in the first approximation we will assume that heat transfer in the calorimeter is determined by the temperature of the capsule T_1 and takes place mainly between the planes of the capsule and the thermal shield. We will also consider the case of moderate values of the absorbed dose (~ 10 kGy), when the increase in the calorimeter temperature does not exceed $\sim 10^\circ\text{C}$ and the change in the thermophysical parameters of the material can be neglected. Due to of the symmetric design of the calorimeter with a closed lid, the heat flux to both sides of the capsule is assumed to be the same. In this case, the heat conduction equation can be represented as:

$$c_1 m_1 \frac{dT_1}{dt} = -\frac{2\lambda_2(T_1 - T_s)}{d}, \quad (4)$$

where c_1 is the heat capacity of the PS-capsule, m_1 is its mass, λ_2 is the thermal conductivity coefficient of the EPS thermal shield, T_s is the temperature of its surface, d is the thickness of the shield ($d = 4.1$ cm).

For the quasi-stationary case, the condition of equality of heat fluxes from the capsule and from the protection surface can be written in the form:

$$c_1 m_1 \frac{dT_1}{dt} = -2\alpha S(T_s - T_0), \quad (5)$$

where α is the heat transfer coefficient on the shield surface, S is the area of the lateral surface of the capsule, T_0 is the ambient temperature. By joint solution of the equations (4) and (5), we obtain:

$$T_1(t) = T_1(0) \exp\left[\frac{2S}{c_1 m_1 (d\lambda_2^{-1} + \alpha^{-1})} t\right] + T_0, \quad (6)$$

where $T_1(0)$ is the steady-state temperature of the capsule immediately after irradiation. Thus, the cooling constant of the capsule with the closed lid is:

$$\tau_c^{\text{closed}} = 0.5c_1 \rho_1^S (d \cdot \lambda_2^{-1} + \alpha^{-1}), \quad (7)$$

where ρ_1^S is the surface density of the capsule.

In turn, for the calorimeter with the removed cover, the main heat flux in the capsule is directed towards its open surface, and the cooling constant takes the form:

$$\tau_c^{\text{open}} = c_1 \rho_1^S (b \cdot \lambda_1^{-1} + \alpha^{-1}), \quad (8)$$

where b is the thickness of the capsule, λ_1 is the coefficient of thermal conductivity of PS.

Table 1 lists some available data on the thermophysical parameters of polystyrene and its modifications.

Table 1

Thermophysical parameters of polystyrene [6]

Parameter	PS	EPS
C, kJ/kg·°C	(1.11...1.33)	$1.65 \cdot 10^3$
λ , W/m·°C	0.165	$(2.8...4.4) \cdot 10^{-2}$
ρ , kg/m ³	(854...1060)	10...200

The heat transfer coefficient α is determined by two processes – convection and radiation. At a temperature of $\sim 30^\circ\text{C}$, the convection makes the main contribution. The α value is ~ 10 W/m²·°C and increases with the increase of the air velocity at the calorimeter surface and the calorimeter temperature. As follows from the formulas (7) and (8), the value of α does not significantly change the estimate of the cooling constant, which is $\sim 1.4 \cdot 10^4$ s for the PS calorimeter with the closed thermal shield and $\sim 3.7 \cdot 10^3$ s with the one opened.

2. STUDY OF THE PYROMETRIC DOSIMETER PROTOTYPE

To test the proposed method, a prototype of the pyrometric dosimeter based on the RISO polystyrene calorimeter [7] and a thermal imager was developed and fabricated.

2.1. MEASUREMENTS WITH THE RISO CALORIMETER

The thermal imager includes a module with an IR sensor type MLX90640, a Raspberry Pi mini-computer, a power supply, a web camera with LED backlight, a temperature and humidity sensor (Fig. 2). The resolu-

tion of the IR sensor is 32×24 pixels, the viewing angle is 55°×45°. The mini-computer runs an I/O controller of an EPICS system [8], and the data from the IR sensor are transmitted to the operator's computer via a local network. The maximal frame rate from the thermal imager is about 8 frames/s. It is also possible to average over frames and write data to a file at a rate of ~1 frame/s. Software is developed using Python scripts and runs in the EPICS system. A Control System Studio package is used as GUI to display information from the thermal imager.

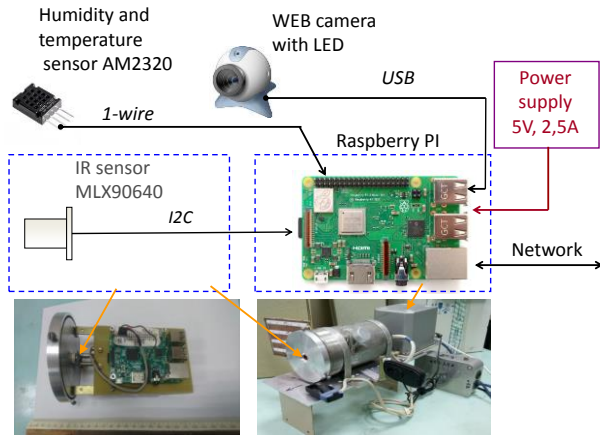


Fig. 2. Block diagram of the thermal imager of the pyrometric dosimeter

2.2. MEASUREMENT PROCEDURE

The studies were carried out on an industrial electron accelerator LU-10 NSC KIPT [9], equipped with a conveyor for the transfer of the processed products to the irradiation zone. The thermal imager was located in the labyrinth of radiation shield of the accelerator behind the turn of the conveyor line at a distance of 55 cm from the front plane of the transport container with the object being processed. Such an object was the RISO calorimeter. The frame size in the front plane of the object was 56×42 cm. The thermistor of the RISO calorimeter was connected via a 4-wire circuit to a multimeter located in the control room. The measurement procedure was as follows:

- The initial temperature of the disk surface of the calorimeter was measured with the lid open before irradiation (~ 10 min).
- The calorimeter with the lid closed was passed through the irradiation zone at a certain conveyor speed and the irradiation time was recorded.
- Then transport container with the calorimeter was moved to the thermal imager to measure the temperature of the latter with the lid closed (~10 min).
- After that, the cover was removed. The temperature on the surface and inside of the calorimeter was measured (~ 30...60 min).

Irradiation of the RISO calorimeter was carried out at a conveyor speed of 3.72, 2.48, 1.24 cm/s. The time between irradiation was ~1 h. During the measurements, the temperature and humidity of the ambient air near the thermal imager were recorded. The absorbed dose was determined by the method [10].

2.3. RESULTS OF THE MEASUREMENTS

Fig. 3,a shows the temperature inside the calorimeter (black square) measured with the thermistor, and the maximum temperature on the surface of the calorimeter disk (red circles) measured with the thermal imager. The moment of irradiation and the moment of opening the calorimeter cover are seen as the temperature jump.

Fig. 3,b demonstrates the averaged temperature of the calorimeter disk surface during cooling and their approximation by function (9). At the initial moment after removing the cover (5...6 min), a transient process of establishing the temperature of the calorimeter is observed.

The temperature inside and on the surface of the cooling calorimeter disk was approximated by an exponential function (see Fig. 3,b):

$$y = A_1 \cdot \exp\left(\frac{-x}{t_1}\right) + y_0, \quad (9)$$

where A_1 is the temperature difference, y_0 is the ambient temperature, t_1 is the time constant (s).

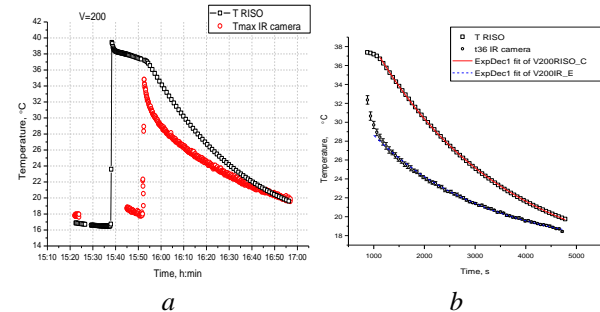


Fig. 3. T_{RISO} – temperature inside the calorimeter (square); $T_{max IR camera}$ – the maximum surface temperature of the calorimeter (circles) during irradiation at a conveyor speed of 1.24 cm/s (a). Temperature of the RISO calorimeter measured with open lid and fitted by an exponential function (b). 136 – average temperature of the calorimeter surface in the center of the disk (circles)

As a result, the dependence of the absorbed dose on the difference in the surface temperature of the RISO calorimeter, measured by the IR camera, was obtained. Table 2 shows the parameters of temperature approximation during cooling of the calorimeter.

Table 2

Parameters of approximation of RISO temperature (RISO) and calorimeter surface temperature (IR)

V conv.	y_0	A_1	t_1
1.24 IR	16.07 ± 0.20	15.15 ± 0.16	2695 ± 72
1.24 RISO	14.15 ± 0.06	23.88 ± 0.04	2567 ± 13
2.48 IR	17.51 ± 0.37	7.22 ± 0.28	1877 ± 192
2.48 RISO	15.30 ± 0.08	13.56 ± 0.07	2895 ± 26
3.72 IR	16.46 ± 2.48	5.17 ± 2.26	2093 ± 1518
3.72 RISO	12.80 ± 0.12	9.51 ± 0.12	3484 ± 55

3. THE MEASUREMENTS WITH THE PHANTOM

3.1. MEASUREMENT PROCEDURE

To test the possibility of using the thermal imager for mapping the dose in an object, the phantom was

irradiated with an electron beam, and the temperature distribution inside the phantom was measured. The phantom consists of 5 stacked plates of expanded polystyrene each by 6.5 cm in thickness t with density of 125 kg/m^3 . On the front plane of the phantom, in the center of each plate, there was a 20 cm long dosimetry film B3 (Fig. 4 on the left) and one more film on the back surface of the last plate. A measuring stand was preliminarily assembled to ensure the fixation of the phantom plates in the field of view of the thermal imager (see Fig. 4 on the right).

The motionless phantom was irradiated with an electron beam scanned in the vertical plane with an energy of 9.3 MeV and an average current 0.73 mA. The scanning amplitude at the exit window was $\pm 8.4 \text{ cm}$, which corresponds to the width of the scanning area on the front surface of the phantom of 47 cm. After irradiation for 15 s, the phantom was removed and moved to the stand (see Fig. 4 on the right)

The surface temperature of each plate was measured for 10 seconds. The interval between measurements was $\sim 1 \text{ min}$. The IR sensor pixel corresponded to a $2.6 \times 2.9 \text{ cm}$ cell on the plate surface.

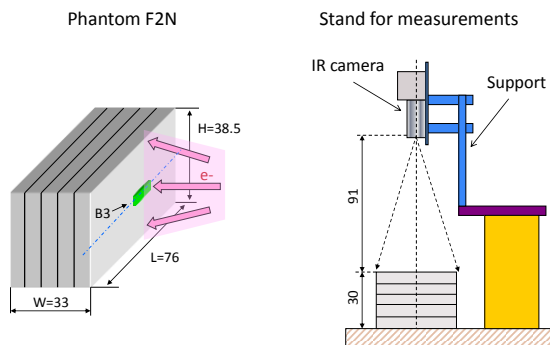


Fig. 4. Phantom (left) and measuring stand (right)

As an example, Fig. 5 shows the temperature distribution on the surface of the 2nd plate.

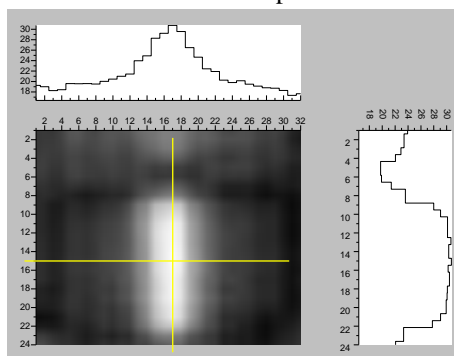


Fig. 5. Surface temperature profiles of the 2nd phantom plate (L2)

3.2. RESULTS OF THE MEASUREMENTS

Data processing from the thermal imager consisted in determining the boundaries of the phantom, building temperature profiles (horizontal and vertical) for each phantom plate.

The obtained horizontal temperature profiles were approximated by a Gaussian in the form:

$$y = y_0 + A \cdot \exp\left(-\frac{1}{2} \left(\frac{x - xc}{w}\right)^2\right), \quad (10)$$

where A is the peak amplitude, y_0 is the displacement along the vertical axis (Y), w is the standard deviation, xc is the position of the peak on the X -axis.

Fig. 6 shows the horizontal temperature profiles and their Gaussian approximation. After approximation, the width of the beam profile along the X -axis, the position and height of the distribution peak were obtained (Table 3). The value of full width at half maximum (FWHM) was calculated using expression:

$$FWHM = 2 \cdot w \cdot \sqrt{\ln(4)} = 2.3548 \cdot w. \quad (11)$$

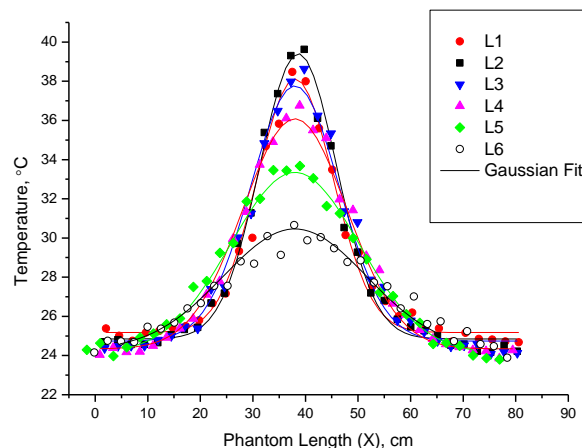


Fig. 6. Horizontal profiles of the surface temperature of phantom plates (L1-L6), solid lines – Gaussian approximation (10)

Table 3

Parameters of approximation by function (10) of the horizontal temperature profile of the phantom plates

No plate	Offset y_0 err <0.19	Center xc err <0.21	SD w err <0.53	Peak Height, A err <0.35	FWHM err <1.2
1	25.18	37.54	7.25	12.94	17.07
2	24.85	38.61	7.30	14.56	17.19
3	24.74	38.00	8.41	13.03	19.81
4	24.34	38.01	9.91	11.74	23.34
5	24.09	37.99	12.20	9.26	28.73
6	24.27	38.00	13.70	6.19	32.26

The absorbed dose was measured with the B3 dosimetry films using a photo scanner (Table 4, Fig. 7).

Table 4

Parameters of approximation of the horizontal dose profile (B3 film) by function (10). The parameter y_0 (offset) was assumed being zero during the approximation

No plate	Center, cm err <0.02	SD, cm err <0.03	Peak Height, kGy err <0.03	FWHM, cm err <0.7
1	38.02	4.95	30.39	11.65
2	37.83	5.39	29.27	12.68
3	37.74	6.09	25.53	14.35
4	38.17	7.36	22.18	17.34
5	38.00	8.86	16.70	20.87
6	38.08	8.39	10.85	19.75

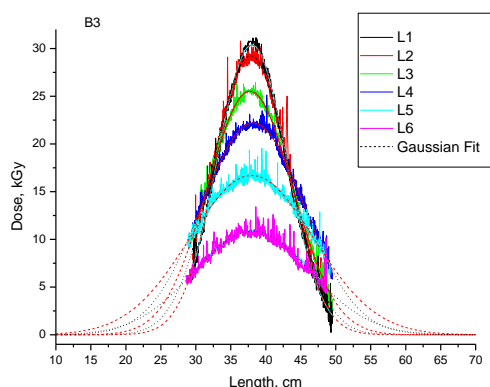


Fig. 7. Dose profiles measured with B3 film and their Gaussian approximations (10)

3.3. COMPUTER SIMULATION

To study of the correctness of restoring the 3D dose distribution in the phantom via the temperature profile after irradiation with a scanned electron beam, the computer simulation of the interaction process of the scanned electron beam and the phantom was carried out using a Geant4 transport code [11]. In the simulations, the radiation parameters corresponded to the actual beam parameters during phantom irradiation.

Fig. 8 shows the distributions of the absorbed dose on the surface of the phantom plates obtained by simulations.

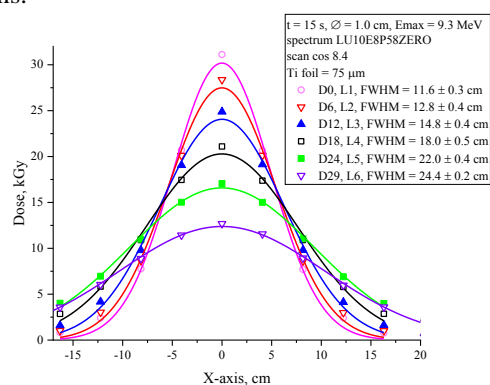


Fig. 8. The distribution of the absorbed dose along the X-axis of phantom (simulations), solid lines – Gaussian approximation

As it can be seen from Table 5, the calculated parameters of the horizontal profile of the absorbed dose and those measured by the B3 film are in good agreement.

Table 5

Parameters of approximation by function (10) of the experimental and calculated dose profiles

No plate	Calculated Peak Height, kGy err<0.8	Calculated FWHM, cm err<0.5	B3 Peak Height, kGy err<0.03	B3 FWHM, cm err <0.7
1	30.2	11.6	30.39	11.65
2	27.5	12.8	29.27	12.68
3	24.1	14.8	25.53	14.35
4	20.3	18.0	22.18	17.34
5	16.6	22.0	16.70	20.87
6	12.4	24.4	10.85	19.75

Fig. 9 shows the dependence of the dose (film B3) on the temperature increment ΔT after irradiation. The measurement result of the first plate was not used in the approximation process as its cooling through the outer surface.

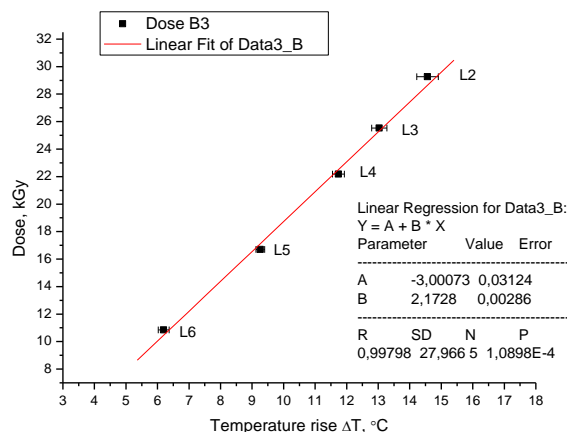


Fig. 9. Dependence of the dose (film B3) on the temperature increment at the surface of the phantom plates (L2-L6) after irradiation (data from Tables 3 and 4) and approximation by a linear function

CONCLUSIONS

1. The panoramic pyrometry method can be used to map the absorbed dose in the phantom made of a material with low thermal conductivity, such as expanded polystyrene, provided that the interval between irradiation of the phantom and temperature measurement is significantly less than the cooling constant of the phantom. The temperature difference inside the phantom before and after irradiation depends linearly on the absorbed dose with a proportionality coefficient of ~ 0.5 deg/kGy.

2. The values of the cooling constant (~ 4 h) obtained in the work on the basis of a simple analytical model are very approximate, taking into account the accepted limitations, as well as the lack of accurate data on the thermophysical characteristics of the material. At the same time, they qualitatively agree with the results of the experiments.

3. Under the conditions of the LU-10 accelerator of NSC KIPT, when a phantom moves from the irradiation zone to the IR camera for ~ 15 min, the decrease in its temperature does not exceed 6...7%. This allows the prompt absorbed-dose mapping in the phantom by the pyrometric technique providing its calibration with the standard film dosimeters.

REFERENCES

- ISO 11137-1:2006/Amd 2:2018 Sterilization of health care products – Radiation – Part 1: Requirements for development, validation and routine control of a sterilization process for medical devices.
- ISO/ASTM 52303:2015 Guide for absorbed-dose mapping in radiation processing facilities. [Electronic resource] Verified 29.04.2021. URL: <https://www.iso.org/ru/standard/67807.html>

3. Ziaie, Farhood & Noori, Abbas. Investigation of high-dose irradiation effects on polystyrene calorimeter response // *Nukleonika*. 2006, v. 51, p. 175.
4. Arne Miller, Andras Kovacs. Calorimetry at industrial electron accelerators // *Nuclear Instruments and Methods in Physics Research Section B: Beam Interactions with Materials and Atoms*. 1985, v. 10-11, Part 2, p. 994-997.
5. U. Gaur and B. Wunderlich. Heat capacity and other thermodynamic properties of linear macromolecules. V. Polystyrene // *Journal of Physical and Chemical Reference Data*. 1982, v. 11, № 2, p. 313-325.
6. George Wypych *PS polystyrene*. Handbook of Polymers 2012 // ChemTec Publishing ISBN 978-1-895198-47-8, p. 541-547.
7. Arne Miller Polystyrene calorimeter for electron beam dose measurements // *Radiation Physics and Chemistry*. 12 Sep. 1995, v. 46, issues 4-6, Part 2, p. 1243-1246.
8. Experimental Physics and Industrial Control System EPICS [Electronic resource] Verified 28.04.2021. URL: <http://www.aps.anl.gov/epics/>
9. V.N. Boriskin, S.A. Vanzha, V.N. Vereshchaka, A.N. Dovbnya, et al. Development of Radiation Technologies and Tests in "Accelerator" Sc&Res Est., NSC KIPT // *Problems of Atomic Science and Technology. Series "Nuclear Physics Investigations"*. 2008, № 5, p. 150-154.
10. ISO/ASTM 51631:2020 Practice for use of calorimetric dosimetry systems for dose measurements and dosimetry system calibration in electron beams.
11. J. Allison, K. Amako, J. Apostolakis, et al. Recent developments in Geant4 // *Nuclear Instruments and Methods in Physics Research Section A: Accelerators, Spectrometers, Detectors and Associated Equipment*. 2016, v. 835, p. 186-225.

Article received 16.02.2022

ПРО МОЖЛИВІСТЬ ЗАСТОСУВАННЯ ПИРОМЕТРИЧНОГО МЕТОДУ В ПРОМИСЛОВІЙ ДОЗИМЕТРІЇ ЕЛЕКТРОННОГО ВИПРОМІНЮВАННЯ

Р.І. Помацалюк, С.К. Романовський, В.О. Шевченко, А.Е. Тенишев, Д.В. Титов, В.Л. Уваров, О.О. Захарченко, В.Ф. Жігло

Валідація процесу стерилізації виробів медичного призначення включає картування просторового розподілу поглинутої дози у фантомі з матеріалу, який є репрезентативний до оброблюваного об'єкту. Зазвичай такі вимірювання проводяться з використанням одноразових хімічних дозиметрів, що розміщені у фантомі у вузлах 3D-сітки. Ця процедура є досить трудомісткою та затратною щодо витрати дозиметричних систем. Вивчена можливість застосування пірометричного методу для оперативного картування поглинутої дози. Дослідження проводилися з використанням прямокутного фантома у вигляді набору пластин з пінополістиролу, на який діє сканований пучок електронів. Проведено спільне вимірювання розподілу температури і поглинутої дози у фантомі. Встановлено лінійну залежність між ними. Розрахунок профілю поглинутої дози виконано також методом МС-моделювання. Показана задовільна відповідність розрахункового розподілу дози з вимірним. Визначено граничні умови застосування запропонованого методу.

О ВОЗМОЖНОСТИ ПРИМЕНЕНИЯ ПИРОМЕТРИЧЕСКОГО МЕТОДА В ПРОМЫШЛЕННОЙ ДОЗИМЕТРИИ ЭЛЕКТРОННОГО ИЗЛУЧЕНИЯ

Р.И. Помацалюк, С.К. Романовский, В.А. Шевченко, А.Э. Тенишев, Д.В. Титов, В.Л. Уваров, А.А. Захарченко, В.Ф. Жигло

Валидация процесса стерилизации продукции медицинского назначения включает картографирование пространственного распределения поглощенной дозы в фантоме из материала, репрезентативного к обрабатываемому грузу. Обычно такие измерения проводятся с использованием одноразовых химических дозиметров, размещаемых в фантоме в узлах 3D-сетки. Эта процедура является весьма трудоемкой и затратной по расходу дозиметрических систем. Изучена возможность применения пиromетрического метода для оперативного картографирования поглощенной дозы. Исследования проводились с использованием прямоугольного фантома в виде набора пластин из пенополистирола, на который воздействует сканируемый пучок электронов. Проведены совместные измерения распределения температуры и поглощенной дозы в фантоме. Установлена линейная зависимость между ними. Расчет профиля поглощенной дозы выполнен также методом МС-моделирования. Показано удовлетворительное соответствие расчетного распределения дозы с измеренным. Определены граничные условия применимости предложенного метода.